HHS Public Access

Author manuscript

Mol Genet Metab. Author manuscript; available in PMC 2023 September 01.

Published in final edited form as:

Mol Genet Metab. 2022 ; 137(1-2): 1–8. doi:10.1016/j.ymgme.2022.06.011.

Growth advantage of corrected hepatocytes in a juvenile model of methylmalonic acidemia following liver directed adeno-associated viral mediated nuclease-free genome editing

Leah E. Venturoni[a,1], **Randy J. Chandler**[a,1], **Jing Liao**[b], **Victoria Hoffmann**[c], **Nikhil Ramesh**[b], **Susana Gordo**[b], **Nelson Chau**[b], **Charles P. Venditti**[a,*]

[a]National Human Genome Research Institute, NIH, Bethesda, MD

[b]LogicBio Therapeutics, Lexington, MA

[c]Office of Research Services, NIH, Bethesda, MD

Abstract

Methylmalonic acidemia (MMA) is a rare and severe inherited metabolic disease typically caused by mutations of the methylmalonyl-CoA mutase (*MMUT*) gene. Despite medical management, patients with MMA experience frequent episodes of metabolic instability, severe morbidity, and early mortality. In several preclinical studies, systemic gene therapy has demonstrated impressive improvement in biochemical and clinical phenotypes of MMA murine models. One approach uses a promoterless adeno-associated viral (AAV) vector that relies upon homologous recombination to achieve site-specific *in vivo* gene addition of *MMUT* into the last coding exon of *albumin (Alb)*, generating a fused *Alb-MMUT* transcript after successful editing. We have previously demonstrated that nuclease-free AAV mediated *Alb* editing could effectively treat MMA mice in the neonatal period and noted that hepatocytes had a growth advantage after correction. Here, we use a transgenic knock-out mouse model of MMA that recapitulates severe clinical and biochemical symptoms to assess the benefits of *Alb* editing in juvenile animals. As was first noted in the neonatal gene therapy studies, we observe that gene edited hepatocytes in the MMA mice treated as juveniles exhibit a growth advantage, which allows them to repopulate the liver slowly but dramatically by 8–10 months post treatment, and subsequently manifest a biochemical and enzymatic response. In conclusion, our results suggest that the benefit of AAV mediated

[*]Correspondence: Charles P. Venditti MD, PhD, Medical Genomic and Metabolic Genetics Branch, National Human Genome Research Institute, National Institutes of Health, Bldg 10, Room 7N248A, Bethesda, MD 20892, Office: 301-496-6213, FAX: 301-402-9056, venditti@mail.nih.gov.

[1]LEV and RJC contributed equally to this work.

Author Contributions

L.E.V., R.J.C., and C.P.V. developed the experimental ideas and design of the study.

Experiments were performed by L.E.V., N.R., J.L., S.G., and N.C. Data analysis was performed by L.E.V., R.J.C., N.R., J.L., S.G., N.C., and V.H. Figures were produced by L.E.V., R.J.C., and C.P.V. The text was written by L.E.V., R.J.C., and C.P.V. with input from all authors. N.C., R.J.C, and C.P.V. supervised the study.

Competing Interest Statement

N.R. and J.L. are employees of LogicBio Therapeutics and receive salary support and stock options from LogicBio Therapeutics. S.G. and N.C. are former employees and shareholders of LogicBio Therapeutics.

nuclease-free gene editing of the *Alb* locus to treat MMA could potentially be therapeutic for older patients.

Keywords

genome editing; gene therapy; methylmalonic acidemia; MMA; fibroblast growth factor 21; FGF21; organic acidemia; adeno-associated virus; AAV; gene editing; selective growth advantage; albumin

1. INTRODUCTION

Methylmalonic acidemia (MMA) is an autosomal recessive inborn error of metabolism most commonly caused by a deficiency of methylmalonyl-CoA mutase (MMUT) [1]. MMUT is a mitochondrially localized enzyme responsible for converting methylmalonyl-CoA to succinyl-CoA. A reduced or complete loss of enzymatic activity results in elevated methylmalonic acid levels in all tissues. Clinically, MMA is a heterogenous multiorgan disease, and the clinical course is characterized by recurrent episodes of life-threatening metabolic crises [2]. Medical management is focused on the dietary restriction of protein and symptomatic management [3–6]. The failure of conventional therapy to improve the outcomes seen in severely affected patients has led to the adoption of elective liver transplantation as a surgical treatment for MMA, with some centers successfully using living related donors to provide the liver to patients less than 1 year of age [7–9]. Although liver transplantation exposes patients to procedural risks and requires life-long immunosuppression, it can prevent metabolic instability and improve quality of life and illustrates the benefits of restored hepatic MMUT activity [9–14]. The promising clinical benefits seen with liver transplantation in MMA patients have helped inspire the development of gene-based therapies to treat MMA in animal models, including AAV based approaches.

Previous work has demonstrated that conventional AAV mediated gene delivery can effectively rescue neonatal mice with the most severe form of MMA [15–21]. However, a rapid loss of hepatic transgene expression was observed, and most of the treated animals developed hepatocellular carcinoma from AAV-mediated insertional mutagenesis of the *Rian* locus [22, 23]. For these reasons, we previously developed a promoterless, nuclease free AAV vector (AAVDJ-Alb-2A-MMUT) designed to express *MMUT* after editing into *Alb* [24–28]. The therapeutic benefit of this approach relies upon successful homologous recombination to target the *MMUT* transgene into the native mouse safe harbor *Alb* locus, just upstream of the stop codon at the 3’ end of this gene (Fig. 1A). After on-target integration, a fused *Alb-2A-MMUT* mRNA is produced under the regulation of the native *Alb* promoter. The 2A peptide sequence mediates ribosomal skipping [29–32] and allows the *Alb-2A-MMUT* mRNA to produce two distinct proteins: ALB-2A and MMUT. Edited *Alb* alleles will produce a circulating Alb-2A protein which can serve as a biomarker of successful recombination.

We previously reported the efficacy, durability, and safety of AAVDJ-Alb-2A-MMUT in two severe mouse models of MMA treated systemically as neonates [28]. Neonatal treated MMA

mice had durable MMUT expression, improved growth with no genotoxicity, in addition to decrease plasma levels of disease biomarkers, FGF21, and methylmalonic acid. Less than 1 percent of the hepatocytes were edited at 2–3 months post-treatment in the MMA mice, which was expected for a gene editing strategy that relies on homologous recombination. However, a significantly higher percentage (12–20%) of corrected hepatocytes was observed at 11–15 months post treatment in the MMA mice but a similar increase was not observed in identically treated control littermates, suggesting the corrected hepatocytes have a selective growth advantage in the setting of MMA. Hepatic MMUT protein expression and the percentage of *MMUT* mRNA expressing hepatocytes were both significantly increased at 11–15 months post treatment, which further supported the observation of a selective growth advantage conferred upon diseased hepatocytes after successful gene editing. The correction of the underlying disease related mitochondrial dysfunction that has been described in both the hepatocytes of MMA mice and patients is hypothesized to be responsible for this growth advantage.

Two important questions that our previous studies did not address are whether this novel gene editing platform to treat MMA could be an effective treatment in older mice and if selection and expansion of corrected MMA hepatocytes might be observed. Here, we demonstrate that AAV-mediated nuclease-free genome editing into *albumin* in a juvenile hypomorphic mouse model of MMA produces a durable and therapeutic expression of MMUT without genotoxicity. In addition, we show that the selective growth advantage previously observed in MMA mice treated as neonates also occurs in older treated MMA animals.

2. MATERIALS AND METHODS:

2.1 Animal Studies.

Animal work was performed in accordance with the National Institutes of Health guide for the care and use of laboratory animals. The mouse model of MMA, $Mmut^{-/-};Tg^{INS\text{-}MCK\text{-}Mmut}$, is maintained on a mixed C57BL/6 × 129SV/Ev × FvBN genetic background as previously described [21]. Mice were fed standard mouse chow (Prolab® RMH 1800) and maintained without special dietary or environmental considerations. Treated mice received a single AAV dose of $1e^{12}$ vector genomes (VG) per mouse (~$7e^{13}$ VG/kg) via retroorbital injection, injected between 44 and 65 days of life. Mice were bled via retro-orbital sinus plexus sampling monthly and frequently weighed. Treated mice were predominantly female (n=10 of 11 treated animals).

2.2 Plasmid Vector and rAAV production.

AAV-Alb-2A-MMUT was generated by replacing the FIX cDNA with a human codon-optimized *MMUT* cDNA from the pAB288 plasmid [24] as previously described [28]. AAVDJ vectors were produced by triple transfection with $Ca_3(PO_4)_2$ followed by CsCl gradient purification [33] and titered as previously described [34].

2.3 Methylmalonic Acid Measurement.

Methylmalonic acid was measured in plasma using gas chromatography-mass spectrometry with stable isotopic internal calibration, as previously described [35].

2.4 Western Blot Analysis.

Samples were prepared and run according to standard protocols. The following antibodies were used for the detection of MMUT (Abcam, ab134956) and ß-Actin (Proteintech, 66009–1-Ig) in conjunction with the following secondary antibodies; (LI-COR, 925–32211), and (LI-COR, 926–68072). Quantification of western blot bands was performed using Image Studio Lite Version 5.2.

2.5 RNA in situ hybridization.

RNAscope probes to detect the human codon-optimized *MMUT* RNA were designed by ACDBio using their proprietary technology and do not cross-react with other mRNAs in the murine transcriptome. Livers were fixed in 4% PFA or 10% NBF and processed into paraffin blocks. Five-micron sections were cut and stained with RNAScope 2.5 HD Assay-Brown (ACDBio 322300) following the manufacturer's instructions. Slide images were captured using an Aperio scanner and quantification was performed using QuPath [36]. Cell detection was performed by detecting the nucleus based on optical density sum. For probe quantification, hepatocytes were divided into the following categories according to probe detection within the cytoplasm: negative; 1+, 1–9 puncta; 2+, 10–19 puncta; or 3+, >20 puncta. Nuclear staining was excluded. An H-score was calculated as follows [1 × (% cells 1+) + 2 × (% cells 2+) + 3 × (% cells 3+)] to generate a score for each sample between 0 and 300 [37].

2.6 Histology and Hepatocellular Carcinoma Screening.

Livers were visually inspected for abnormalities at necropsy, then fixed in formalin, embedded, serially sectioned, stained with hematoxylin and eosin, and reviewed by a veterinary pathologist.

2.7 Vector Genome Quantitation.

Genomic DNA from liver samples was extracted using DNeasy Blood & Tissue Kit (Qiagen; 69506). ddPCR was performed according to the manufacturer's recommendations for the BioRad QX200 AutoDG ddPCR system using 10 ng or 20 ng of DNA as input and the following probes: BIO-RAD ddPCR CNV assay *Gapdh* (Cat # 10042961, dMumCNS300520369) and *MMUT* (Cat # 10042958 dCNS513322846).

2.8 Albumin Integration Assay.

Genomic DNA from liver samples was extracted using DNeasy Blood & Tissue Kit (Qiagen; 69504). Genomic integration was determined by PCR amplification from upstream of the 5' integration site to the 2A element (F: 5'-ATGTTCCACGAAGAAGCCA-3', R: 5'-TCAGCAGGCTGAAATTGGT-3) followed by qPCR quantification (F: 5'-ATGTTCCACGAAGAAGCCA-3', R: 5'-AGCTGTTTCTTACTCCATTCTCA-3', Probe:

5’AGGCAACGTCATGGGTGTGACTTT-3’). A synthesized DNA fragment representing this product was used to generate a standard curve as previously described [28].

2.9 ELISAs.

ALB-2A in plasma was measured by chemiluminescence sandwich ELISA using a proprietary rabbit polyclonal anti-2A antibody for capture and HRP-labelled anti-mouse albumin for detection. FGF21 protein was measured using an ELISA kit (Abcam, ab212160) per the manufacturer’s instructions.

2.10 Statistical analyses.

Prism 8 by GraphPad was used to analyze all data. Results are expressed as mean ± SEM. Values of $p<0.05$ were considered statistically significant. Depending on the experimental design, an unpaired t-test, log-rank (Mantel-Cox) test, or simple linear regression was used as indicated in the legends of the figures.

3. RESULTS

3.1 Treatment and Survival

Mmut$^{-/-}$;*Tg*$^{INS\text{-}MCK\text{-}Mmut}$ (MMA mice) maintained on standard mouse chow were used to study AAV mediated *Alb* editing. This transgenic mouse model of MMA uses the muscle creatine kinase promoter (MCK) to express a murine *Mmut* transgene exclusively in the skeletal and cardiac muscle [21]. Mutant mice exhibit increased morbidity and mortality, growth retardation, elevated plasma MMA (pMMA), and elevated plasma FGF21 compared to unaffected, wildtype littermates. The survival of mutant mice is highly dependent on diet and environmental stress. Eleven two-month-old MMA mice received a retro-orbital injection of the AAVDJ-Alb-2A-MMUT vector at a dose of $1e^{12}$ vector genomes (VG) per mouse (~$7e^{13}$ VG/kg). This dose was selected to match the dose used in our previous study in neonates and to facilitate comparisons between studies. The survival of treated and untreated MMA mice is shown in Fig. 1B. Treatment did not significantly increase the survival of the MMA mice ($p=0.57$; (Mantel-Cox) test). In the treated group (n=11), 3 mice died within days of high stress events, such as a cage flood or following retro-orbital injection, and 1 was sacrificed due to declining health at 4 months post therapy which pathology revealed to be likely unrelated to MMA pathophysiology or AAV treatment. After injection 4 animals were sacrificed at 2 months, and the remaining 3 animals were sacrificed 8 to 10 months post treatment to assess the therapeutic effects.

3.2 Weight and Disease-Associated Plasma Biomarkers

The animals were evaluated monthly for weight gain and disease plasma biomarkers, including plasma methylmalonic acid (pMMA) and FGF21. MMA mice were significantly runted before treatment (mean weight = 12.6g ± 0.8 at 2 months vs. wildtype mean weight = 21.9g ± 0.7 at 2 months) and did not display increased weight gain compared to untreated MMA mice for the duration of the study ($p=0.68$ at 8 months; unpaired t-test) (Supplemental fig. 1). pMMA was significantly reduced ($p<0.05$; unpaired t-test) at 2- and 8-months post treatment (4 and 10 months of age) compared to age matched untreated mutant mice (Fig. 1C). At 10 months, treated mutants had an average pMMA of 536μM ± 157 (n=3)

compared to age-matched untreated mutants average pMMA of 1150 μM ± 149 (n=7) (p=0.04; unpaired t-test).

Plasma FGF21 levels, hypothesized to reflect mitochondrial dysfunction, are known to be elevated in MMA mice and human patients [21]. Treatment with AAVDJ-Alb-2A-MMUT significantly (p<0.001; unpaired t-test) reduced plasma levels of FGF21 in the juvenile mice (mean = 3.5ng/mL ± 0.78, n=8) compared to untreated mutant mice (mean = 34.8ng/mL ± 5.8, n=5) (Fig. 1D). FGF21 levels were reduced within 1 month of treatment and remained low for the duration of the study (Supplemental Fig 2).

3.3 Hepatic MMUT Expression and Vector Integration

Hepatic MMUT in wildtype control mice, untreated and treated MMA mice was measured by immunoblotting. Protein expression was detected in 2 of 5 MMA animals at 2 to 4 months post treatment (4 animals sacrificed at 2 months and 1 due to declining health at 4 months) and all 3 MMA animals at 8 to 10 months post treatment but not in untreated MMA animals (Fig. 2A). Western blot results were quantified as a percentage of MMUT and normalized to ß-actin expression (Fig. 2B). Treated MMA mice at 8 to 10 months post-treatment had significantly higher levels of MMUT (80% ± 39.1) compared to 2 to 4 months posttreatment (3.4% ± 2.7; p<0.05; unpaired t-test).

Viral copy number in the liver was determined by the ratio of *MMUT* genome copies to *Gapdh* copies by ddPCR. There was not a significant difference in the number of viral genomes at 2 to 4 months post treatment (8.9 ± 2.9 genomes) compared to 8 to 10 months post treatment (4.0 ± 2.0 genomes) (p=0.28; unpaired t-test) (Fig. 2C). To determine the integration frequency of *MMUT* into the *Alb* locus, we performed a semi-quantitative PCR measurement. Amplification was performed across the recombination site (from the 2A element, through the 5' arm of homology, to upstream of the 5' homology arm) and quantified by qPCR as previously described [28] (Supplemental Fig. 3A and 3B). For each mouse, DNA was isolated from two distinct regions of the liver and assayed for integrations. The average of the technical replicates showed that treated MMA mice had significantly more *MMUT* integrations into the *Alb* loci at 8 to 10 months post treatment (3.42% ± 2.2) as compared to 2 to 4 months post treatment (0.18% ± 0.32) (p<0.05; unpaired t-test; Fig. 2D and Supplemental fig. 3C).

Corrected hepatocytes produce a 21 amino acid 2A peptide fused to the 3' terminus of albumin (Fig. 1A), which can be detected in the plasma. When AAVDJ-Alb-2A-MMUT was used to treat MMA mice in the neonatal period, the plasma ALB-2A levels correlated with integration frequency and hepatic protein expression [28]. MMA mice treated as juveniles also have increased levels of plasma ALB-2A, which continue to increase over time (Fig. 2E). The maximum level of plasma ALB-2A detected in each mouse remained a small component of the total albumin produced, with ALB-2A levels never exceeding 3% of the total plasma ALB levels. A linear regression analysis indicated that plasma ALB-2A levels highly correlate with hepatic MMUT protein expression (r^2=0.9192, p<0.0005) (Fig. 2F) and were associated with integration events (r^2=0.4712, p=0.06).

Livers from treated mice were stained for *MMUT* mRNA expression and localization by immunohistochemistry. The total number of corrected hepatocytes was quantified by QuPath [36] for each image and demonstrates significant variability between mice the same age post-treatment; however, on average all treated mice show around 20% of hepatocytes were corrected regardless of time post-treatment (Fig. 3A). While the total number of corrected hepatocytes did not vary on average regardless of time post treatment; the pattern of corrected cells was distinct when comparing mice sacrificed shortly after treatment (2 months post treatment, Fig. 3B and 3C) to those sacrificed later (8 months post treatment, Fig. 3D and 10 months post treatment, Fig. 3E). At 2 months post treatment, only isolated individual cells show staining, with no pattern of corrected vs. uncorrected cells (Fig. 3B and 3C). In contrast, at 8- and 10-months post-treatment, corrected cells show a pattern of large, distinct clusters, which is characteristic of clonal expansion of an edited cell (Fig. 3D and 3E). Livers were also stained by H&E and examined by a veterinary pathologist. All examined sections appeared morphologically normal, and no signs of dysplasia or cancer were detected in any of the treated animals.

4. DISCUSSION

MMA is a debilitating multisystemic disorder that remains difficult to manage with the current standard of care. It has been established that MMUT plays an important role in most tissues throughout the body [20], and widespread correction could have a theoretical benefit to treat MMA. However, observations from murine mouse models of MMA with tissue specific expression of MMUT [38] as well as treatment of various murine models of MMA with both constitutive and tissue specific canonical AAV gene therapy vectors [15–18, 39] demonstrate that hepatic expression of MMUT substantially ameliorates disease symptomatology. In addition, observations from patients who receive elective liver transplants demonstrate a reduction of plasma methylmalonic acid levels and a dramatic improvement in metabolic stability [9], providing hope that liver targeted gene therapy with a durable, integrating transgene might deliver similar benefits without the procedural risks associated with transplantation or the need for lifelong immune suppression afterward. We previously demonstrated that AAV vectors utilizing targeted integration into hepatocytes safely and effectively could treat a variety of mouse models of MMA when administered to animals in the neonatal period [28, 40]. In all models, we repeatedly observed a growth advantage conferred upon hepatocytes corrected with targeted, integrating MMUT vectors. In the case of AAVDJ-Alb-2A-MMUT treatment of neonates, this selective advantage allows for the initial, low level of integration to generate a large population of corrected hepatocytes over time. Previous work did not address if this approach would be an effective treatment in older mice or if the treatment of older mice would allow for the selection and expansion of corrected MMA hepatocytes.

Here, we find that clonal expansion of corrected hepatocytes due to selective advantage is variable but present when mice are treated as young adults. Although we had a small number of older treated mice in our study, we consistently observed that MMA mice with the highest levels of plasma ALB-2A also had the highest percentages of *Alb* integration, more hepatic MMUT production, reduced pMMA, and had more corrected hepatocytes by immunohistochemistry. As seen with neonatal treatment using the same mouse model, the

plasma ALB-2A levels correlate with the percentage of *Alb* integrations, highlighting the utility of this circulating biomarker for longitudinal assessment of editing and in vivo hepatic expansion.

Elevated plasma FGF21 levels in MMA patients have been associated with worsening disease manifestations and correlate with abnormal hepatic mitochondrial ultrastructure [21]. Importantly, MMA patients who have received a liver or combined liver and kidney transplant have dramatically reduced plasma FGF21 levels compared to pretransplant levels. Treatment of MMA mice with a 3' *Alb* integrating vector quickly and dramatically reduced plasma FGF21, similar to what has been noted after administration with a canonical AAV8 MMUT vector [21], suggesting that even the very low levels of *Alb* editing mediated by AAVDJ-Alb-2A-MMUT at early times might mitigate mitochondrial dysfunction.

Treatment of juvenile MMA mice with AAVDJ-Alb-2A-MMUT did not affect mortality, despite pronounced hepatic correction seen at later times. It is essential to highlight that the survival of this strain of MMA mice is highly dependent on diet and environmental stress. In fact, Manoli *et al.* noted an 87% survival at day of life 120 when mice were kept on a diet containing 21% protein supplemented with carbohydrate rich fruit and Nutrical® and heating strips to reduce temperature fluctuations [21]. However, the same mice exhibit a 43% survival at day 120 of life when maintained on a regular murine diet at ambient temperatures in the setting of standard housing [28]. Because AAVDJ-Alb-2A-MMUT editing relies upon natural HR, which is inefficient, especially in older mice, the mice succumb to the natural history of MMA before an expression benefit of MMUT can be realized. Future efforts should be directed toward either increasing AAV mediated HR using small molecules, such as the ribonucleotide reductase inhibitor fludarabine, or with nuclease enhancement, as demonstrated for Crigler Najjar syndrome. [41, 42].

The results here, and those previously published, support the concept that the underlying hepatopathy of MMA provides an environment that allows a cell autonomous growth advantage to manifest as an edited cell becomes "protected" against the effects of the disease. An increased turnover of uncorrected hepatocytes is also posited, which leads us to speculate that a pool of mitotically active hepatocytes exists to match the demand for hepatocyte turnover in MMA. This pool of replicating hepatocytes would be amenable to AAV mediated HR and perhaps explains the successful editing we document in MMA mice treated as juveniles when liver doubling has ceased. The pattern of MMUT expression in older mice appears as random clusters, which is consistent with clonal proliferation after correction and not with zonulation.

The dosage of AAV used in this study was selected because it is similar to what was administered to neonatal mice in our previous publication (2.5e13 vg/kg to 2.5e14 vg/kg) [28]. However, high doses of AAV are proving to be feasible in an FDA approved therapy for SMA type 1 (1.1e14 vg/kg), and an ongoing phase I/II clinical trial to treat patients with MMA (NCT04581785) using a humanized version of the vector which proposes to treat patients with a dose of 5e13 vg/kg, followed by escalation to 5e14 vg/kg. Dose finding studies in the ongoing phase I/II clinical trial will be critical to define the kinetics of clonal

expansion of corrected hepatocytes that might occur in MMA patients after treatment with an analogous, humanized integrating AAV vector [43].

Supplementary Material

Refer to Web version on PubMed Central for supplementary material.

Acknowledgments

L.E.V., R.J.C., and C.P.V. were supported by the Intramural Research Program of the National Human Genome Research Institute. This work was completed with assistance from the National Cancer Institute Pathology/Histotechnology Laboratory and the CCR Genomics Core. We owe special thanks to Andrew Warner and Elijah Edmondson for their aid in performing RNAscope and analysis. We would also like to acknowledge Darwin Romero for assistance with tracking animals and data entry. This work was funded, in part, by LogicBio Therapeutics, Inc.

FINANCIAL SUPPORT

This work was funded by the Intramural Research Program of the National Human Genome Research Institute and, in part, by LogicBio Therapeutics, Inc.

ABBREVIATIONS

MMA	methylmalonic acidemia
MMUT	methylmalonyl-CoA mutase
AAV	adeno-associated virus
FGF21	fibroblast growth factor 21
Alb	albumin
VG	vector genomes
MCK	muscle creatine kinase promoter
pMMA	plasma methylmalonic acid

References

[1]. Manoli I, Sloan JL, Venditti CP. Isolated Methylmalonic Acidemia. In: Adam MP, Ardinger HH, Pagon RA, Wallace SE, Bean LJH, Stephens K, et al., editors. GeneReviews((R)). Seattle (WA); 1993.

[2]. Matsui SM, Mahoney MJ, Rosenberg LE. The natural history of the inherited methylmalonic acidemias. The New England journal of medicine 1983;308:857–861. [PubMed: 6132336]

[3]. Baumgartner MR, Horster F, Dionisi-Vici C, Haliloglu G, Karall D, Chapman KA, et al. Proposed guidelines for the diagnosis and management of methylmalonic and propionic acidemia. Orphanet J Rare Dis 2014;9:130. [PubMed: 25205257]

[4]. Fraser JL, Venditti CP. Methylmalonic and propionic acidemias: clinical management update. Curr Opin Pediatr 2016;28:682–693. [PubMed: 27653704]

[5]. Hauser NS, Manoli I, Graf JC, Sloan J, Venditti CP. Variable dietary management of methylmalonic acidemia: metabolic and energetic correlations. Am J Clin Nutr 2011;93:47–56. [PubMed: 21048060]

[6]. Manoli I, Myles JG, Sloan JL, Shchelochkov OA, Venditti CP. A critical reappraisal of dietary practices in methylmalonic acidemia raises concerns about the safety of medical foods. Part 1: isolated methylmalonic acidemias. Genet Med 2016;18:386–395. [PubMed: 26270765]

[7]. Sloan JL, Manoli I, Venditti CP. Liver or combined liver-kidney transplantation for patients with isolated methylmalonic acidemia: who and when? The Journal of pediatrics 2015;166:1346–1350. [PubMed: 25882873]

[8]. Spada M, Calvo PL, Brunati A, Peruzzi L, Dell'Olio D, Romagnoli R, et al. Liver transplantation in severe methylmalonic acidemia: The sooner, the better. The Journal of pediatrics 2015;167:1173.

[9]. Niemi AK, Kim IK, Krueger CE, Cowan TM, Baugh N, Farrell R, et al. Treatment of methylmalonic acidemia by liver or combined liver-kidney transplantation. The Journal of pediatrics 2015;166:1455–1461 e1451. [PubMed: 25771389]

[10]. Chen PW, Hwu WL, Ho MC, Lee NC, Chien YH, Ni YH, et al. Stabilization of blood methylmalonic acid level in methylmalonic acidemia after liver transplantation. Pediatr Transplant 2010;14:337–341. [PubMed: 19686300]

[11]. Pillai NR, Stroup BM, Poliner A, Rossetti L, Rawls B, Shayota BJ, et al. Liver transplantation in propionic and methylmalonic acidemia: A single center study with literature review. Mol Genet Metab 2019;128:431–443. [PubMed: 31757659]

[12]. Sakamoto R, Nakamura K, Kido J, Matsumoto S, Mitsubuchi H, Inomata Y, et al. Improvement in the prognosis and development of patients with methylmalonic acidemia after living donor liver transplant. Pediatr Transplant 2016;20:1081–1086. [PubMed: 27670840]

[13]. Chu TH, Chien YH, Lin HY, Liao HC, Ho HJ, Lai CJ, et al. Methylmalonic acidemia/propionic acidemia - the biochemical presentation and comparing the outcome between liver transplantation versus non-liver transplantation groups. Orphanet J Rare Dis 2019;14:73. [PubMed: 30940196]

[14]. Vernon HJ, Sperati CJ, King JD, Poretti A, Miller NR, Sloan JL, et al. A detailed analysis of methylmalonic acid kinetics during hemodialysis and after combined liver/kidney transplantation in a patient with mut (0) methylmalonic acidemia. Journal of inherited metabolic disease 2014;37:899–907. [PubMed: 24961826]

[15]. Carrillo-Carrasco N, Chandler RJ, Chandrasekaran S, Venditti CP. Liver-directed recombinant adeno-associated viral gene delivery rescues a lethal mouse model of methylmalonic acidemia and provides long-term phenotypic correction. Hum Gene Ther 2010;21:1147–1154. [PubMed: 20486773]

[16]. Chandler RJ, Venditti CP. Long-term rescue of a lethal murine model of methylmalonic acidemia using adeno-associated viral gene therapy. Molecular therapy : the journal of the American Society of Gene Therapy 2010;18:11–16. [PubMed: 19861951]

[17]. Chandler RJ, Venditti CP. Pre-clinical efficacy and dosing of an AAV8 vector expressing human methylmalonyl-CoA mutase in a murine model of methylmalonic acidemia (MMA). Mol Genet Metab 2012;107:617–619. [PubMed: 23046887]

[18]. Senac JS, Chandler RJ, Sysol JR, Li L, Venditti CP. Gene therapy in a murine model of methylmalonic acidemia using rAAV9-mediated gene delivery. Gene Ther 2012;19:385–391. [PubMed: 21776024]

[19]. Chandler RJ, Zerfas PM, Shanske S, Sloan J, Hoffmann V, DiMauro S, et al. Mitochondrial dysfunction in mut methylmalonic acidemia. FASEB journal : official publication of the Federation of American Societies for Experimental Biology 2009;23:1252–1261. [PubMed: 19088183]

[20]. Chandler RJ, Sloan J, Fu H, Tsai M, Stabler S, Allen R, et al. Metabolic phenotype of methylmalonic acidemia in mice and humans: the role of skeletal muscle. BMC Med Genet 2007;8:64. [PubMed: 17937813]

[21]. Manoli I, Sysol JR, Epping MW, Li L, Wang C, Sloan JL, et al. FGF21 underlies a hormetic response to metabolic stress in methylmalonic acidemia. JCI Insight 2018;3.

[22]. Chandler RJ, LaFave MC, Varshney GK, Burgess SM, Venditti CP. Genotoxicity in Mice Following AAV Gene Delivery: A Safety Concern for Human Gene Therapy? Molecular

therapy : the journal of the American Society of Gene Therapy 2016;24:198–201. [PubMed: 26906613]

[23]. Chandler RJ, LaFave MC, Varshney GK, Trivedi NS, Carrillo-Carrasco N, Senac JS, et al. Vector design influences hepatic genotoxicity after adeno-associated virus gene therapy. J Clin Invest 2015;125:870–880. [PubMed: 25607839]

[24]. Barzel A, Paulk NK, Shi Y, Huang Y, Chu K, Zhang F, et al. Promoterless gene targeting without nucleases ameliorates haemophilia B in mice. Nature 2015;517:360–364. [PubMed: 25363772]

[25]. Porro F, Bortolussi G, Barzel A, De Caneva A, Iaconcig A, Vodret S, et al. Promoterless gene targeting without nucleases rescues lethality of a Crigler-Najjar syndrome mouse model. EMBO Mol Med 2017;9:1346–1355. [PubMed: 28751579]

[26]. Borel F, Tang Q, Gernoux G, Greer C, Wang Z, Barzel A, et al. Survival Advantage of Both Human Hepatocyte Xenografts and Genome-Edited Hepatocytes for Treatment of alpha-1 Antitrypsin Deficiency. Molecular therapy : the journal of the American Society of Gene Therapy 2017;25:2477–2489. [PubMed: 29032169]

[27]. Nygaard S, Barzel A, Haft A, Major A, Finegold M, Kay MA, et al. A universal system to select gene-modified hepatocytes in vivo. Sci Transl Med 2016;8:342ra379.

[28]. Chandler RJ, Venturoni LE, Liao J, Hubbard BT, Schneller JL, Hoffmann V, et al. Promoterless, nuclease-free genome editing confers a growth advantage for corrected hepatocytes in mice with methylmalonic acidemia. Hepatology (Baltimore, Md) 2020.

[29]. Donnelly MLL, Luke G, Mehrotra A, Li X, Hughes LE, Gani D, et al. Analysis of the aphthovirus 2A/2B polyprotein ‘cleavage’ mechanism indicates not a proteolytic reaction, but a novel translational effect: a putative ribosomal ‘skip’. The Journal of general virology 2001;82:1013–1025. [PubMed: 11297676]

[30]. Sharma P, Yan F, Doronina VA, Escuin-Ordinas H, Ryan MD, Brown JD. 2A peptides provide distinct solutions to driving stop-carry on translational recoding. Nucleic acids research 2012;40:3143–3151. [PubMed: 22140113]

[31]. Johnson LA, Morgan RA, Dudley ME, Cassard L, Yang JC, Hughes MS, et al. Gene therapy with human and mouse T-cell receptors mediates cancer regression and targets normal tissues expressing cognate antigen. Blood 2009;114:535–546. [PubMed: 19451549]

[32]. Kim JH, Lee SR, Li LH, Park HJ, Park JH, Lee KY, et al. High cleavage efficiency of a 2A peptide derived from porcine teschovirus-1 in human cell lines, zebrafish and mice. PLoS One 2011;6:e18556.

[33]. Grimm D, Lee JS, Wang L, Desai T, Akache B, Storm TA, et al. In vitro and in vivo gene therapy vector evolution via multispecies interbreeding and retargeting of adeno-associated viruses. J Virol 2008;82:5887–5911. [PubMed: 18400866]

[34]. Nakai H, Thomas CE, Storm TA, Fuess S, Powell S, Wright JF, et al. A limited number of transducible hepatocytes restricts a wide-range linear vector dose response in recombinant adeno-associated virus-mediated liver transduction. J Virol 2002;76:11343–11349. [PubMed: 12388694]

[35]. Marcell PD, Stabler SP, Podell ER, Allen RH. Quantitation of methylmalonic acid and other dicarboxylic acids in normal serum and urine using capillary gas chromatography-mass spectrometry. Anal Biochem 1985;150:58–66. [PubMed: 4083484]

[36]. Bankhead P, Loughrey MB, Fernandez JA, Dombrowski Y, McArt DG, Dunne PD, et al. QuPath: Open source software for digital pathology image analysis. Sci Rep 2017;7:16878. [PubMed: 29203879]

[37]. Ishibashi H, Suzuki T, Suzuki S, Moriya T, Kaneko C, Takizawa T, et al. Sex steroid hormone receptors in human thymoma. J Clin Endocrinol Metab 2003;88:2309–2317. [PubMed: 12727990]

[38]. Manoli I, Sysol JR, Li L, Houillier P, Garone C, Wang C, et al. Targeting proximal tubule mitochondrial dysfunction attenuates the renal disease of methylmalonic acidemia. Proc Natl Acad Sci U S A 2013;110:13552–13557. [PubMed: 23898205]

[39]. Li L, Chandler RJ, Andres-Mateos E, Xiao R, Ilyinskii P, Vandenberghe LH, et al. Anc80 and AAV8 Vectors Mediate Equivalent Long-Term Hepatic Correction of Methylmalonyl-CoA Mutase Deficiency in a Murine Model of Methymalonic Acidemia (MMA). MOLECULAR

THERAPY; 2018: CELL PRESS 50 HAMPSHIRE ST, FLOOR 5, CAMBRIDGE, MA 02139 USA; 2018. p. 450–450.

[40]. Schneller JL, Lee CM, Venturoni LE, Chandler RJ, Li A, Myung S, et al. In vivo genome editing at the albumin locus to treat methylmalonic acidemia. Molecular therapy Methods & clinical development 2021;23:619–632. [PubMed: 34901307]

[41]. Tsuji S, Stephens CJ, Bortolussi G, Zhang F, Baj G, Jang H, et al. Fludarabine increases nuclease-free AAV- and CRISPR/Cas9-mediated homologous recombination in mice. Nature biotechnology 2022.

[42]. De Caneva A, Porro F, Bortolussi G, Sola R, Lisjak M, Barzel A, et al. Coupling AAV-mediated promoterless gene targeting to SaCas9 nuclease to efficiently correct liver metabolic diseases. JCI insight 2019;5:e128863.

[43]. Lisowski L, Dane AP, Chu K, Zhang Y, Cunningham SC, Wilson EM, et al. Selection and evaluation of clinically relevant AAV variants in a xenograft liver model. Nature 2014;506:382–386. [PubMed: 24390344]

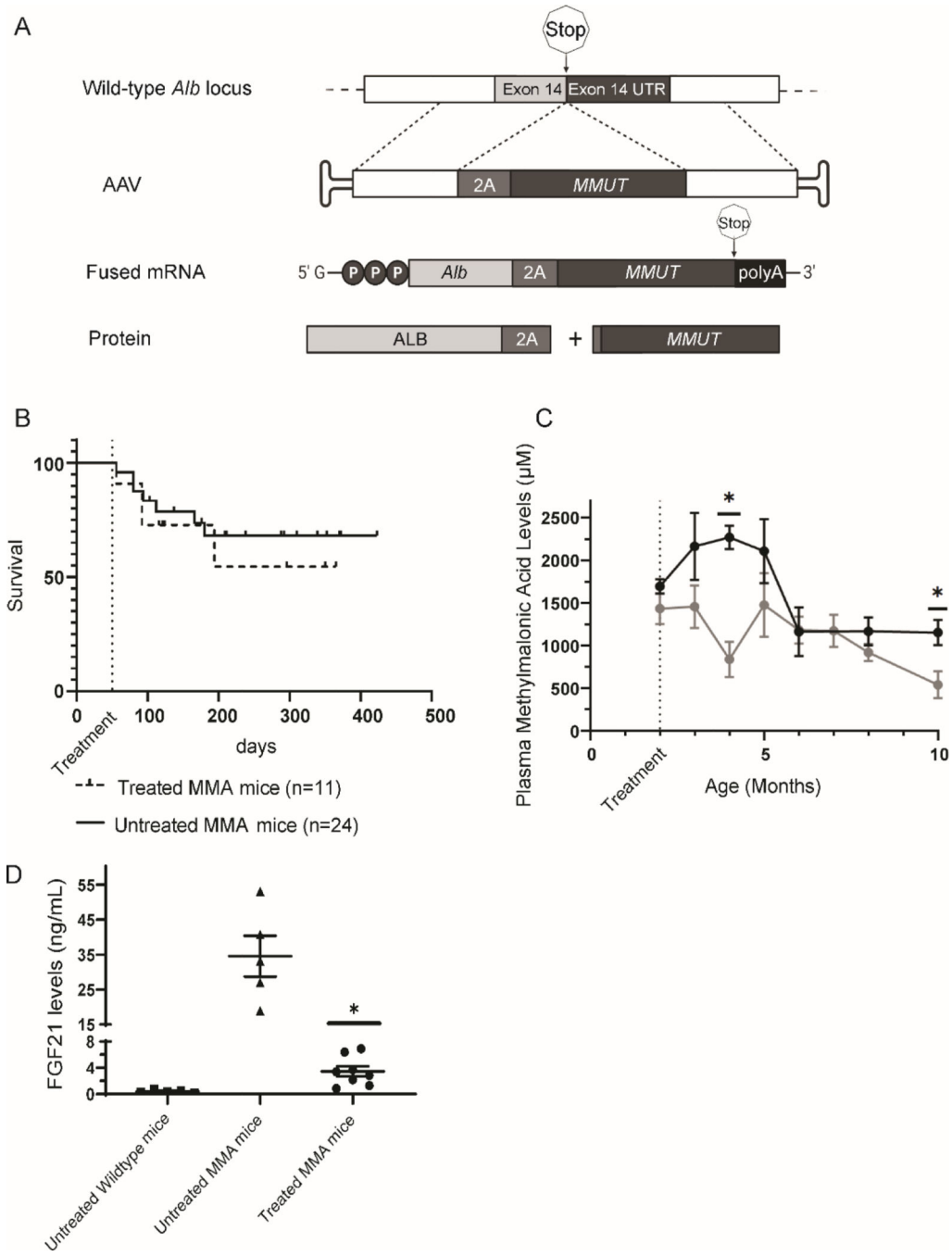

Fig 1. AAVDJ-Alb-2A-MMUT treatment and response in MMA mice.

A. A schematic of AAVDJ-Alb-2A-MMUT integration and expression. An AAV containing the 2A-MMUT sequenced flanked by arms of homology to either side of the stop codon of *Alb* is delivered to hepatocytes in the liver-tropic AAVDJ capsid. Homologous recombination between the native murine *Alb* locus and the AAV generates a fused *Alb-2A-MMUT* allele under the control of the native *Alb* promoter, producing a fused mRNA. 2A mediated self-cleavage produces two distinct proteins, ALB-2A and MMUT, where the start methionine of MMUT has been replaced with proline. Only edited alleles will produce

ALB-2A. **B.** Survival of mice treated at two months of age (n=11) was not significantly different from untreated MMA mice (n=24) (p=0.57; (MantelCox) test). **C.** Treated MMA mice (n= 11, 10, 7, 4, 4, 3, 2, 3, 3) have reduced levels of plasma methylmalonic acid (pMMA) compared to untreated MMA mice (n= 11, 10, 5, 8, 5, 0, 7, 0, 7) with a significant reduction at 4 and 10 months of age (*p<0.05; unpaired t-test). The dotted line at 2 months represents when the mice were treated. Error bars are ± the SEM. **D.** Treated MMA mice (n=8) had significantly reduced plasma FGF21 levels compared to untreated MMA mice (n=5) (*p<0.0001; unpaired t-test).

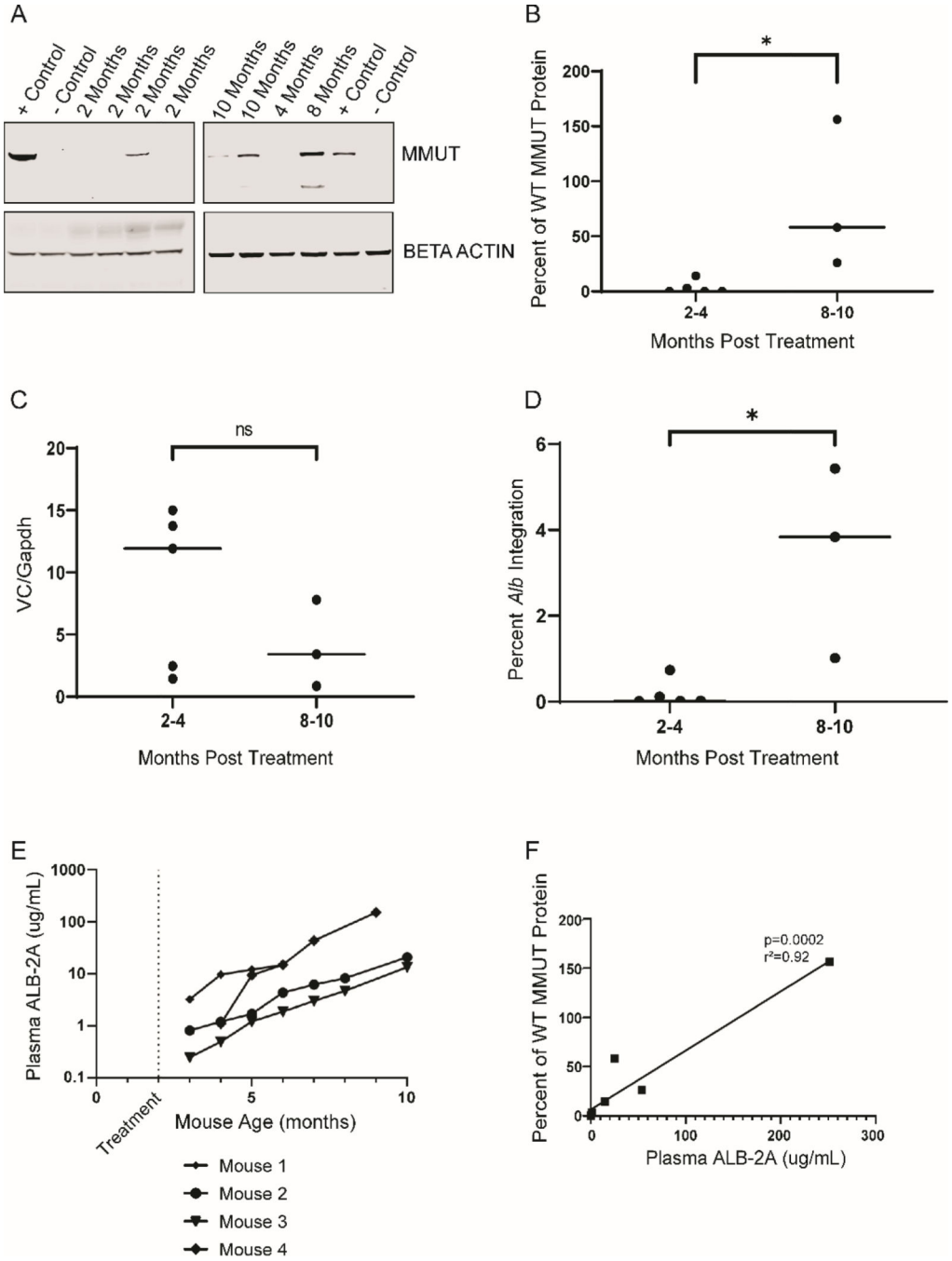

Figure 2. Characterization of hepatic editing following treatment with AAVDJ-Alb-2A-MMUT.

A. Immunoblot of hepatic MMUT protein (85 kDa) expression in wildtype mice (+ Control), untreated MMA mice (− Control), and treated MMA mice at 2-, 10-, 4- and 8-months post treatment. ß-actin (42 kDa) was used as a loading control. **B.** Hepatic MMUT protein expression was quantified as a percentage of wildtype MMUT protein expression and normalized to ß-actin expression. (*p<0.05; unpaired t-test) **C.** Viral copy number represented as the ratio of *MMUT* genome copies to *Gapdh* copies as determined by ddPCR. (p=0.28; unpaired t-test) **D.** The percent of hepatic *Alb* alleles with MMUT integrations in

two distinct liver regions as determined by semi-quantitative PCR. (*$p<0.05$; unpaired t-test) **E.** Plasma ALB-2A levels over time in 4 treated MMA mice. **F.** A simple linear regression of plasma ALB-2A level and the percent of wildtype MMUT protein expression.

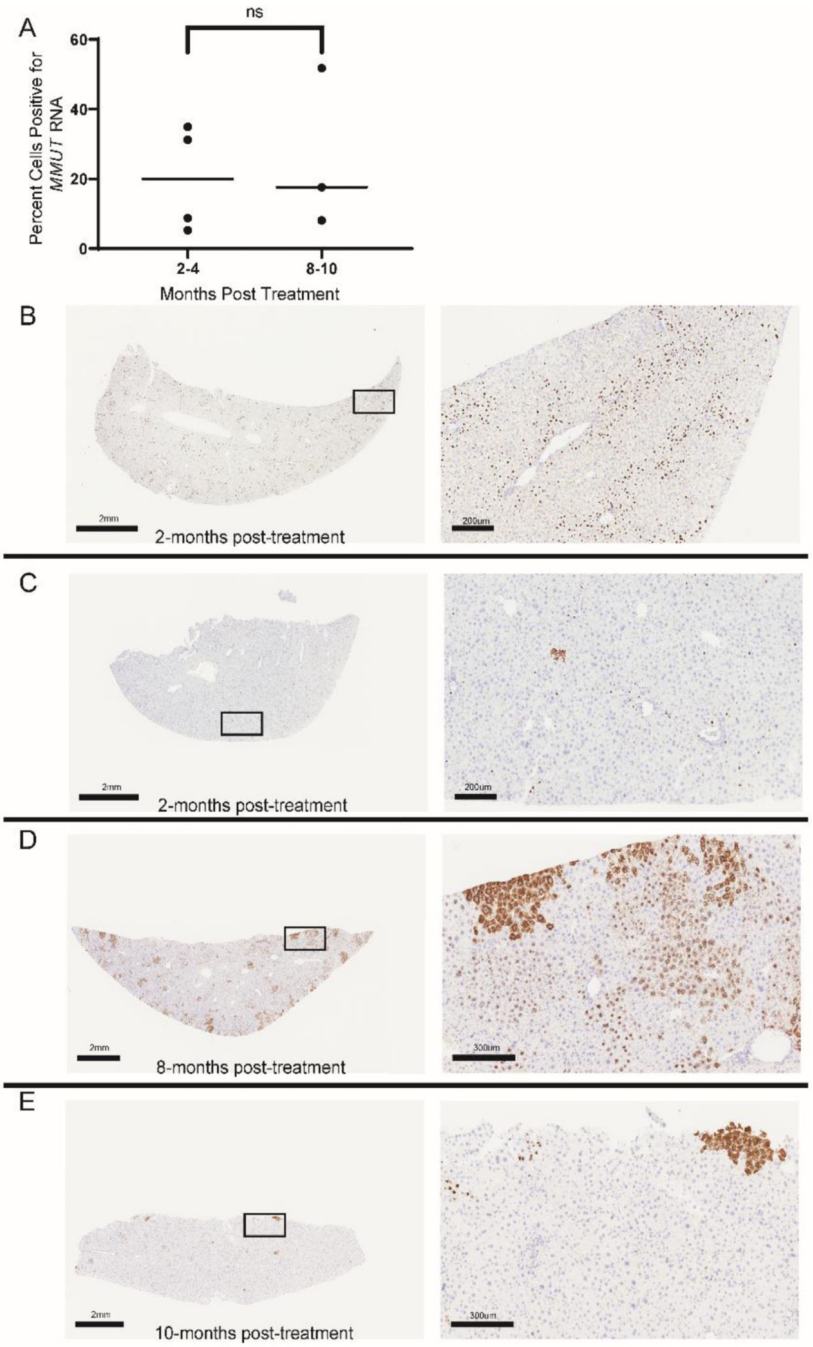

Figure 3. *MMUT* mRNA expression in edited hepatocytes.

A. The percentage of cells stained for *MMUT* mRNA in treated mice. **B-E.** Representative mRNA *in situ* hybridization images of treated MMA mice. Cells positive for *MMUT* mRNA are stained brown. The scale bar is 2mm, and the insert (right image) is a 10x magnification. **B-C.** Representative images from mice 2-months post treatment. **D.** Representative images from a mouse 8-months post treatment. **E.** Representative images from a mouse 10-months post treatment.